V International Conference on Particle-based Methods – Fundamentals and Applications
PARTICLES 2017
P. Wriggers, M. Bischoff, E. Oñate, D.R.J. Owen, & T. Zohdi (Eds)

ON THE EFFECT OF STATIC AND DYNAMIC PARTICLE SIZE DISTRIBUTION ON FLOW TURBULENCE MODULATION

DERRICK O. NJOBUENWU[1] AND MICHAEL FAIRWEATHER[2]

School of Chemical and Process Engineering, University of Leeds
Leeds, LS2 9JT, United Kingdom
[1]d.o.njobuenwu@leeds.ac.uk; [2]m.fairweather@leeds.ac.uk

Key words: Large eddy simulation, Discrete particle simulation, Gravity, Turbulence modulation, Agglomeration, Particle size distribution.

Abstract. The effect of an evolving particle size distribution due to particle agglomeration and breakup, and the direction and absence of gravitational acceleration, on flow turbulence modulation is investigated using large eddy and discrete particle simulation of a turbulent channel flow. The results are compared with the case in which the particle size distribution is static and where only inter-particle collision is allowed. Due to the small particle Stokes number considered, inherent in a solid-liquid flow, and the small simulation time, only small effects were observed for the static versus dynamic particle size distribution on the fluid turbulence. For vertical channel flows, however, the influence of flow direction and gravity lead to different particle segregation patterns which, together with changes in wall shear stresses and mass flow rate due to buoyancy effects, do affect the flow turbulence and the evolution of inter-particle collisions, collision efficiency and agglomerate breakup.

1 INTRODUCTION

The structures in a turbulent flow are known to be highly complex, associated with time-dependent, three-dimensional phenomena covering a wide range of spatial and temporal scales. The degree of the complexity increases with the introduction of a dispersed particle phase. Additional effects include the interaction between phases in terms of mass, momentum and energy (as applicable) exchange, the interaction between particles and any walls, and the influence of gravity, particle collision, agglomeration and breakup. Since the system performance is a complex function of such underlying phenomena, a detailed knowledge regarding the hydrodynamics and the evolution of the dispersed phase is essential for understanding such systems. The governing features of the dispersed phase are its size and velocity distributions, both of which have a major influence on the flow turbulence.

Previous works have focused on the effect of particle size distribution (PSD) on fluid turbulence. These have been performed by studying two-way coupling and four-way coupling [1, 2], where the effects of two-way coupling between the particles and the flow, and inter-particle collisions, on fluid turbulence are considered. To the best of our knowledge, there has been no work on the effect of an evolving PSD due to particle agglomeration and breakup on turbulence modulation. Work to date therefore considered the effect of a static, poly-dispersed PSD on turbulence modulation. In this paper, an eddy-resolving simulation for prediction of

the fluid velocity distribution is adopted to improve confidence in the results. Large eddy simulation (LES) is preferred to direct numerical simulation (DNS) to benefit from LES's lower computational cost as compared to DNS. Discrete particle simulation (DPS) considering particle drag, shear-lift, pressure gradient, added mass and buoyancy forces, and sub-grid scale velocity fluctuation contributions to particle acceleration, is applied to treat the particle dynamics in the turbulent flow. The classical particle-in-cell technique is used to treat the two-way coupling.

Most numerical simulations exclude the gravitational force to study only turbulence-induced agglomeration. However, gravitational acceleration is inevitably present and hence must be included as one of the external forces that induce particle-particle interactions leading to agglomeration and sedimentation. The inclusion of gravitational acceleration does alter the fluid mass flow rate and the particle behaviour in a system, as shown in the literature [3-5].

In resolving four-way coupling aspects, the search for possible binary particle collisions is based on a deterministic method following domain decomposition. The outcome of all collisions is determined using a hard-sphere collision model while all collisions are subjected to an energy-balance agglomeration to test for possible agglomeration [6]. All agglomerates are subjected to hydrodynamic shear stresses in the flow for possible breakup of agglomerates [7]. Note that agglomerate breakup is due to agglomerate-agglomerate or primary particle-agglomerate collisions, and through impact with a wall or due to hydrodynamic shear [7].

The LES-DPS developed for predicting the dynamic PSD and turbulence modulation is tested on flows of relevance to the transport of nuclear waste sludge. Channel flow is the simulation domain while calcite particles suspended in water are the nuclear waste simulant. Results will be presented in terms of the PSD, and profiles of fluid and particle velocities, with simulation time, focussing on the impact of the evolving particle size distribution on the flow turbulence.

2 MATHEMATICAL FORMULATION

A four-way coupled Eulerian-Lagrangian approach is adopted since the suspension is dense with high particle volume fractions. In large eddy simulation, the continuity and Navier-Stokes equations are spatially filtered so that the energy-containing large-scale turbulent motions are solved while the sub-grid scales (SGS) are modelled. The filtered governing equations with the influence of the dispersed phase can be expressed as:

$$\frac{\partial \bar{u}_j}{\partial x_j} = 0 \tag{1}$$

$$\frac{\partial \bar{u}_i}{\partial t} + \frac{\partial \bar{u}_i \bar{u}_j}{\partial x_j} = -\frac{1}{\rho}\frac{\partial \bar{p}}{\partial x_i} + \frac{\partial}{\partial x_j}\left(\bar{\sigma}_{ij} - \tau_{ij}\right) + \frac{\Pi}{\rho} + \frac{S_{m,i}}{\rho} \tag{2}$$

where $\bar{\sigma}_{ij} = -2\nu\bar{S}_{ij}$ represents the viscous stress, $\bar{S}_{ij} = 0.5(\partial\bar{u}_i/\partial x_j + \partial\bar{u}_j/\partial x_i)$ is the filtered strain-rate tensor, ν is the kinematic viscosity, $\tau_{ij} = \overline{u_i u_j} - \bar{u}_i\bar{u}_j$ is the SGS tensor which represents the effect of the SGS motions on the resolved motions, t is time, x_j is the spatial co-ordinate directions, u_j is the velocity vector, p is the pressure, and ρ is the density. The SGS tensor is computed using the dynamic version of the Smagorinsky model proposed by Piomelli and Liu [8]. Its specific implementation has been presented in a recent paper [9]. $\Pi = -\rho u_\tau^2/h$ is the mean pressure constant imposed along the streamwise direction (z-axis)

that drives the flow. $S_{m,i}$ is a source term and accounts for the action on the fluid of the particles, given by the sum of all hydrodynamic forces in the momentum equation due to all particles in a fluid computational cell.

The motion of a particle in a turbulent flow field follows Newton's second law of motion:

$$\mathrm{d}\mathbf{v} = \left\{ \frac{(\bar{\mathbf{u}} - \mathbf{v})}{\tau_p} f_D + C_{SL} \frac{3\rho}{4\rho_p} [(\bar{\mathbf{u}} - \mathbf{v}) \times \bar{\boldsymbol{\omega}}] + \frac{\rho}{\rho_p} \frac{\mathrm{D}\bar{\mathbf{u}}}{\mathrm{D}t} + \frac{\rho}{2\rho_p} \left(\frac{\mathrm{d}\bar{\mathbf{u}}}{\mathrm{d}t} - \frac{\mathrm{d}\mathbf{v}}{\mathrm{d}t} \right) + \left(1 - \frac{\rho}{\rho_p} \right) \mathbf{g} \right\} \mathrm{d}t \tag{3}$$

$$\mathrm{d}\mathbf{x_p} = \mathbf{v}\mathrm{d}t \tag{4}$$

An important notation convention is that the derivatives $\mathrm{d}/\mathrm{d}t$ and $\mathrm{D}/\mathrm{D}t$ represent Lagrangian derivatives, following the particle and the containing fluid element respectively, so that boldface symbols denote the vector quantities, with $\mathrm{d}\bar{\mathbf{u}}/\mathrm{d}t = \partial\bar{\mathbf{u}}/\partial t + \mathbf{v} \cdot \nabla\bar{\mathbf{u}}$ and $\mathrm{D}\bar{\mathbf{u}}/\mathrm{D}t = \partial\bar{\mathbf{u}}/\partial t + \bar{\mathbf{u}} \cdot \nabla\bar{\mathbf{u}}$. The terms on the right-hand side of Eq. (3) are, respectively, contributions from the drag, shear lift, pressure-gradient, added-mass, and buoyancy forces. The particle properties are denoted by the subscript p, and fluid properties are either given without a subscript (for readability) or by the subscript f (where it enhances clarity). $\mathbf{v}$ and $\mathbf{x_p}$ are the particle instantaneous velocity and position; $\bar{\mathbf{u}}$ and $\bar{\boldsymbol{\omega}} = 0.5(\nabla \times \bar{\mathbf{u}})$ are known resolved fluid velocities and rotation interpolated at particle position. The term f_D is a non-linear correction due to the particles' finite Reynolds number, $Re_p = |\bar{\mathbf{u}} - \mathbf{v}| d_p/\nu$, taken from the Schiller and Naumann drag correlation, and expressed as $f_D = 1.0 + 0.15 Re_p^{0.687}$, with d_p as the particle diameter. $\tau_p = (\Phi_p d_p^2)/18\nu$ is the particle relaxation time and when normalised by the viscous time-scale $\tau_f = \nu/u_\tau^2$, gives the particle Stokes number, $\tau_p^+ = \tau_p/\tau_f$, which is then used to characterise the particle response time, with $\Phi_\rho = \rho_p/\rho$ being the particle to fluid density ratio. Hence, a superscript $(^+)$ denotes variables made dimensionless in wall (viscous) units using the fluid kinematic viscosity, ν, and the fluid shear velocity, u_τ. The shear lift force coefficient C_{SL} accounts for corrections due to small and large particle Reynolds numbers, as proposed by Mei [10].

The deterministic hard-sphere collision model [11] is adopted to treat the interactions between particles due to binary collisions. Agglomeration for the colliding particles is based on an expression which permits agglomeration if the elastic energy (i.e. the relative kinetic energy before the collision minus the dissipated energy) after the compression period of the collision is less than the work required to overcome the van der Waals' forces [12]:

$$\frac{(\mathbf{v}_2^- - \mathbf{v}_1^-)^2 - [(\mathbf{v}_2^- - \mathbf{v}_1^-) \cdot \mathbf{n}_\mathrm{c}]^2 (1 - e_n^2)}{|(\mathbf{v}_2^- - \mathbf{v}_1^-) \cdot \mathbf{n}_\mathrm{c}|} \leq \frac{H^*}{6\delta_0^{*2}} \left[(1 - e_n^2) \frac{6}{\pi^2 \rho_p^* \bar{p}^*} \frac{d_{p,1}^{*3} + d_{p,2}^{*3}}{d_{p,1}^{*2} d_{p,2}^{*2} (d_{p,1}^* + d_{p,2}^*)} \right]^{1/2} \tag{5}$$

where quantities with the superscript * are made dimensionless in the integral scale using the channel half-height h, bulk velocity, u_b and fluid density, ρ. H is the particle Hamaker constant, $\bar{p}$ is the maximum contact pressure at which plastic deformation occurs, δ_0 is the minimal contact distance and e_n is the normal restitution coefficient. Note the superscript $(^-)$ denotes quantities before the collision, and the subscripts 1 and 2 denote particles number one and two. The agglomerate size and structure are based on a volume-equivalent sphere.

Breakup is defined as a singular event in time, i.e. there is an exact moment in time when an agglomerate turns from being intact into being broken. We assume that this happens when the local hydrodynamic stress $\sigma \sim \mu(\epsilon/\nu)^{1/2}$ at the agglomerate position, acting on the

agglomerate, exceeds a critical stress, σ_{cr} [7]; where ϵ is the instantaneous turbulence kinetic energy dissipation rate at the position of the agglomerate, and μ and ν are the dynamic and kinematic viscosities. The critical stress σ_{cr} is a characteristic of the considered agglomerate, i.e. σ_{cr} is a function of the aggregate properties such as size, structure, type of the constituting particles, and the chemical environment. Among these variables, the size of the aggregate is most crucial. A large body of experimental, numerical and theoretical studies, see Babler et al. [7] and cited references, suggest a power law dependency of the form:

$$\sigma_{cr} \sim r^{-q} = N_{pp}^{-q/d_f} \tag{6}$$

where $N_{pp} \sim r^{d_f}$ is the number of primary particles constituting the agglomerate, d_f is the agglomerate fractal dimension, r is the radius of the primary particle, and $q = \left[9.2\left(3 - d_f\right) + 1\right]/2$ is a scaling exponent that depends on the agglomerate structure [7]. There are no exact models to effect breakup, and recent research [7] has been limited to detecting the moment break-up events are likely to occur. We adopt this model for detecting breakup events for small agglomerates and subsequently breakup the parent agglomerate into two daughter particles. This method of breaking an agglomerate into two parts is a popular modelling assumption mainly because of the lack of data for other types of breakup mode.

3 NUMERICAL SIMULATIONS

The BOFFIN-LES code [13] was used to solve the LES equations. The shear Reynolds number of the channel flow was $Re_\tau = u_\tau\, h/\nu = 300$ based on the properties of water ($\rho = 1000$ kg m^{-3}, $\nu = 10^{-6}$ m^2 s^{-1}). The computational domain, $2h \times \pi h \times 2\pi h$, was discretised using grid nodes of $129 \times 128 \times 128$ in the wall normal, spanwise and streamwise directions, respectively. Periodic boundary conditions are applied in the streamwise and spanwise directions and the no-slip condition is imposed on the walls.

Table 1: Calcite mechanical properties and influence of particle diameter, normal restitution coefficient and volume fraction on particle-particle interactions.

Parameter	Symbol	Unit	Value
Particle density	ρ_p	kg m^{-3}	2710
Hamaker constant	H	J	3.8×10^{-20}
Mean yield stress	$\bar{p}$	Pa	3.0×10^{8}
Minimal contact distance	δ_0	m	2.0×10^{-10}
Particle diameter	d_p	μm	60
Normal restitution coefficient	e_n	-	0.4
Particle volume fraction	α_p	-	1×10^{-3}

Particles are injected uniformly into the fully developed un-laden flow with their velocity set to the local fluid velocity and tracked by solving the particle equation of motion. A 4th-order Runge-Kutta scheme and a trilinear interpolation scheme are employed in the DPS code with time step equal to that of the LES. Periodic boundary conditions are applied in the streamwise and spanwise directions and perfect elastic collisions are imposed on the walls.

The particle simulation properties and the mechanical properties of calcite particles, a simulant for UK legacy waste sludge, used in these simulations are listed in Table 1. Particle-particle collisions are considered within a long dispersion phase to assure a proper mixing of the primary particles. Then, two-way coupling, inter-particle collision, agglomeration and breakup are considered. The instant in time at which the agglomeration and breakup models are applied is denoted $t^* = 0$ and then a dimensionless time interval of $\Delta t^* \sim 100$ is investigated.

4 RESULTS AND DISCUSSION

Figure 1 shows the population balance (growth and/or death) of the single, N_{pp}, and agglomerate particles, $N_{a,i\leq 5}$, defined as the ratio of the number of particle sizes to the initial number of total single particles, $N_0 = 2{,}748{,}100$, after a simulation time $t^* = tu_b/h = 100$. In this test case, agglomeration and breakup were monitored for primary particles with particle diameter, $d_p = 60$ μm, particle Stokes number, $\tau_p^+ = 5$, density ratio, $\rho_p/\rho \sim 100$ and agglomerate fractal dimension, $d_f = 2.0$.

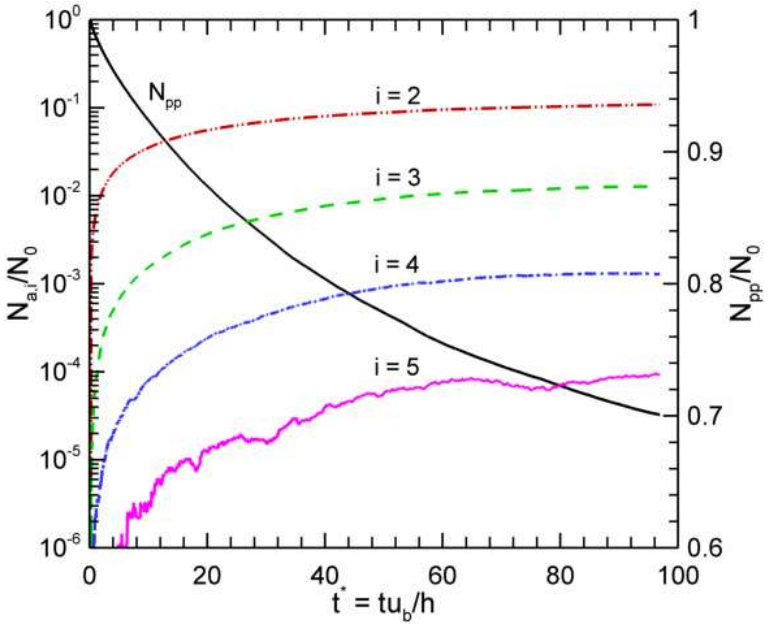

Figure 1: Time evolution of the population of single, N_{pp}, and agglomerate particles, $N_{a,i=2,3,\ldots}$. Lines are as follows: black (−) single; red (− ·· −) double; green (− −) triple; blue (− · −) quadruple; purple (−) quintuple

Figure 1 shows the particle size distribution at any time instance, t^*, and demonstrates that agglomerates of two particles, $N_{a,i=2}$, form first. With increasing time, large agglomerates begin to form through collisions between single particles and larger agglomerates, and between the agglomerates themselves, all constrained by de-agglomeration due to hydrodynamic shear stress acting on the agglomerate. The rate of formation and breakup of

the lower order agglomerates, e.g. $N_{a,i=2,3}$, ultimately tends to a steady state, while those of the higher order agglomerates, e.g. $N_{a,i=5}$, show an unsteady trend since the large agglomerates are susceptible to breakup.

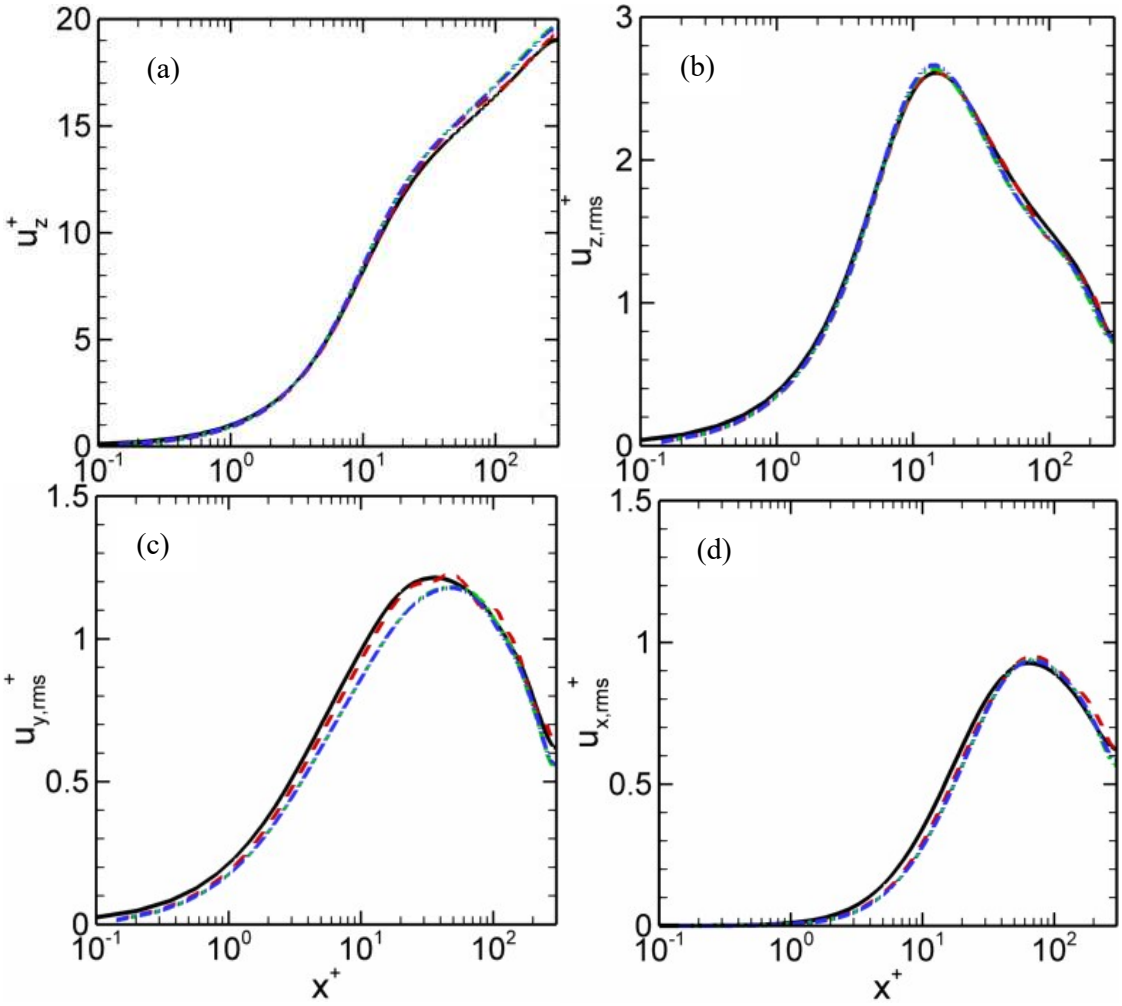

Figure 2: (a) Mean streamwise fluid velocity, u_z^+, and rms of fluid velocity fluctuations for (b) streamwise, $u_{z,\mathrm{rms}}^+$, (c) spanwise, $u_{y,\mathrm{rms}}^+$, and (d) wall-normal, $u_{x,\mathrm{rms}}^+$, components. Lines are as follows: black (−) unladen DNS; red (− −) unladen LES; green (− · −) four-way coupled LES, with collision only and blue (− ·· −) four-way coupled LES, with collision, agglomeration and breakup ($d_p = 60$ µm, $\rho_p/\rho \sim 100$, $\tau_p^+ = 5$, $d_f = 2.0$).

Following the test case presented in Figure 1 where four-way coupling including inter-particle collision, agglomeration and breakup are considered, the first and second statistical turbulent moments for the liquid phase are compared in Figure 2 with those obtained from unladen DNS [14], unladen LES and four-way coupled LES with inter-particle collision only, all computed at shear Reynolds number $Re_\tau = 300$. The four-way coupling case considering particle collision, agglomeration and breakup results in a dynamic particle size distribution,

while the four-way coupling case considering inter-particle collision only results in a static PSD, and in this case mono-dispersity.

Figure 2 gives profiles of the mean streamwise fluid velocity, u_z^+, and the root mean square (rms) of the fluid velocity fluctuations in the streamwise, $u_{z,\mathrm{rms}}^+$, spanwise, $u_{y,\mathrm{rms}}^+$, and wall-normal, $u_{x,\mathrm{rms}}^+$, directions. All show only small differences between the unladen flow and the four-way coupled case based on the static and dynamic PSDs. Although the presence of particles in the fluid flow does modulate the flow turbulence, therefore, the degree of this modulation depends on several factors as reviewed in Pang et al. [15]. Due to a small particle Stokes number, $\tau_p^+ = 5$, for this flow, and a small elapsed simulation time $\Delta t^* \sim 100$, the consideration of two-way coupling with static and dynamic PSD has little effect on the fluid statistical moments studied. This negligible effect of small particle Stokes number on fluid statistics has been observed in previous studies, e.g. [12].

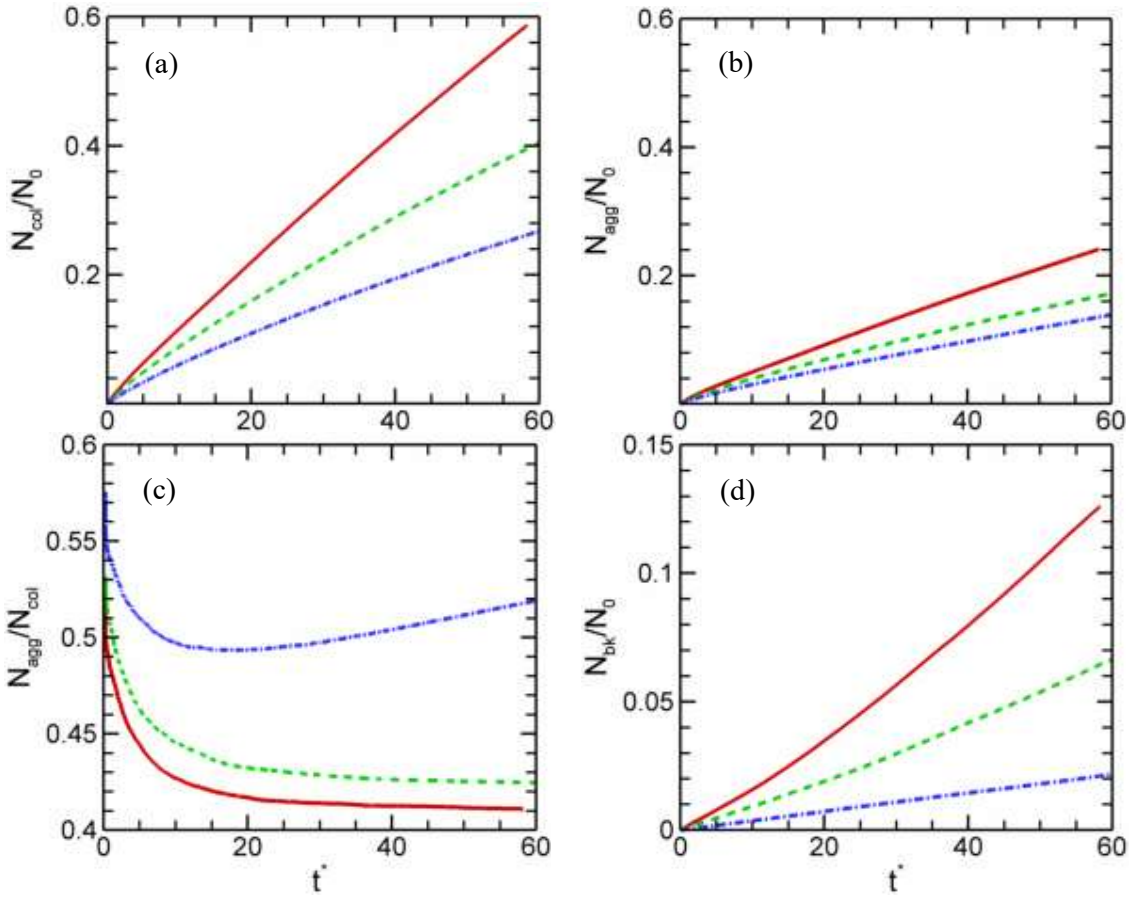

Figure 3: Time history of (a) the total number of the accumulated particle-particle collisions, N_{col}/N_0, (b) the total number of the accumulated particle-particle collisions leading to agglomeration, N_{agg}/N_0 , (c) the agglomeration rate, N_{agg}/N_{col}, and (d) the total number of the accumulated agglomerate breakups, N_{bk}/N_0; N_0 is the total number of primary particles $\left(d_p = 60\ \mu m,\ \rho_p/\rho = 2.71\right)$ initially injected into the domain. Lines are as follows: red (−) downward flow; green (− −) no-gravity flow; and blue (− · −) upward flow.

Figure 3 shows the evolution of the number of collisions, N_{col}, the number of collisions which satisfy the agglomeration criterion in Eq. (5), N_{agg}, the agglomeration rate, N_{agg}/N_{col}, and the number of breakups, N_{bk}, for the three flows considered, i.e. downward flow, no-gravity flow and upward flow, all normalised by the initial total number of primary particles, $N_0 = 2{,}748{,}100$. The effect of momentum exchange between the solid and liquid phases, the shear induced lift force and the direction of gravity all have an effect on particle segregation, inter-particle collision, particle agglomeration and agglomerate breakup. Subsequently, their combined effects influence the fluid first and second statistical moments.

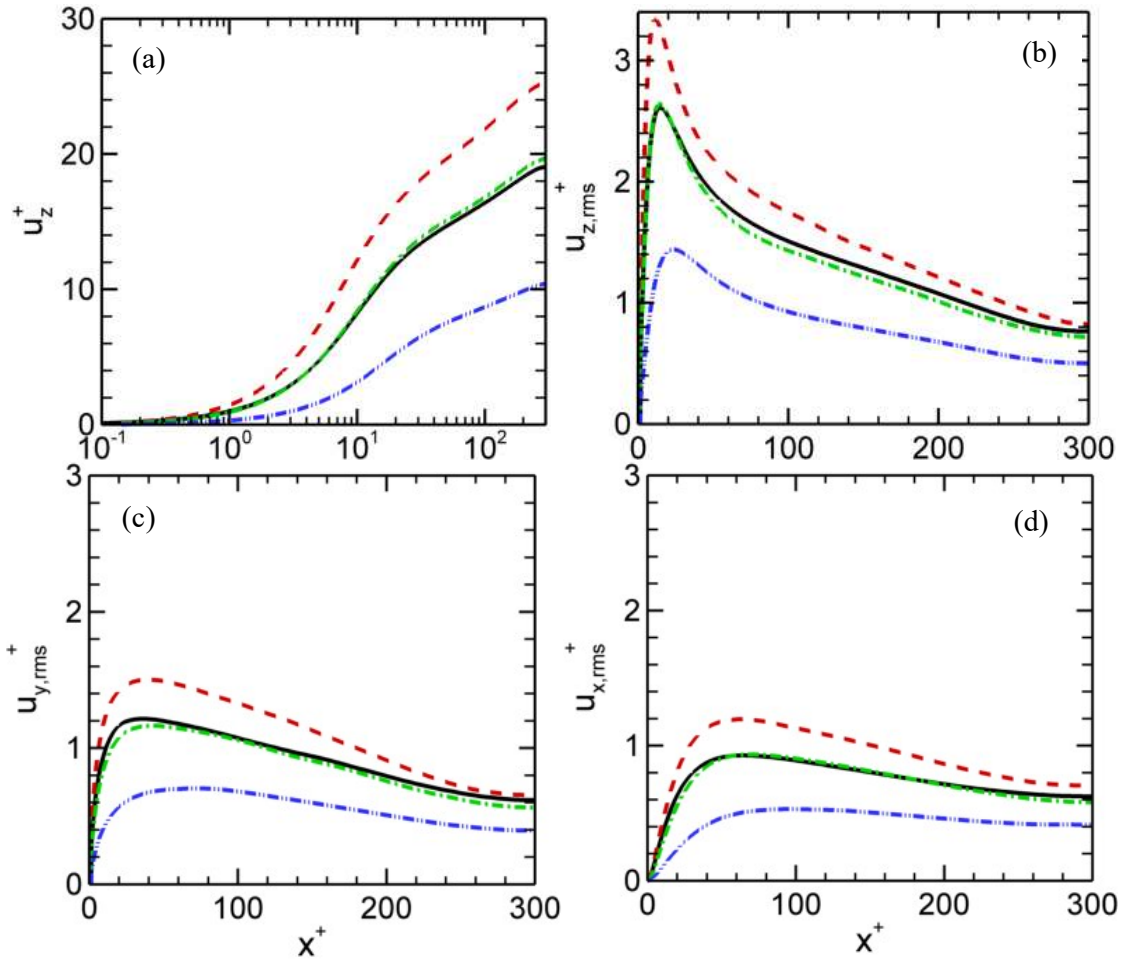

Figure 4: (a) Mean streamwise fluid velocity, u_z^+, and rms of fluid velocity fluctuations for (b) streamwise, $u_{z,\mathrm{rms}}^+$, (c) spanwise, $u_{y,\mathrm{rms}}^+$, and (d) wall-normal, $u_{x,\mathrm{rms}}^+$, components. Simulations based on particle diameter $d_p = 60$ μm and $\rho_p/\rho = 2.71$ Lines are as follows: black (−) unladen DNS; red (− −) downward flow; green (− · −) no-gravity flow; and blue (− ·· −) upward flow.

The particles in the downward flow (DF) and no-gravity flow (NG) accumulate at the wall, with the former showing more particle segregation at the wall compared to the flow without gravity. In contrast to both these flows, the particles in the upward flow (UF) are depleted in the near-wall region. Note the results that support this observation are not shown here, but this has been observed previously [2]. Due to presence of gravity, and also to local momentum exchange with the carrier fluid and to differences in particle segregation, we observe in Figure 4 significant increases (resp. decreases) of both the wall shear and liquid mass flow rate in downward (resp. upward) flows when compared to the no-gravity flow. Hence, in the three cases, the particles see significantly different turbulence intensities, as is evident in the evolution of the number of collisions, agglomerations, breakups and the agglomeration rate in Figure 3. With the largest wall shear stress and mass flow rate for the downward flow, the DF case showed the highest rate of particle collisions, N_{col}/N_0, agglomeration events, N_{agg}/N_0, and breakups, N_{bk}/N_0. In contrast, the DF case showed the lowest agglomeration rate, N_{agg}/N_{col}. These observations are consistent with theory and with our earlier observations reported in Njobuenwu and Fairweather [6], where particle collision, agglomeration and breakup, all increased, while the agglomeration rate (N_{agg}/N_{col}) decreased, with an increase in the carrier-phase mass flow rate (Reynolds number). Hence, the influence of the direction of gravity in a vertical flow on particle collision, agglomeration and breakup is like that of flow Reynolds number, i.e. equivalent to increased Reynolds number of DF, and decreased for UF. In the same vain, the UF showed the least particle collision, agglomeration and breakup, but the largest agglomeration rate.

5 CONCLUSIONS

The effect of the particle size distribution (static versus dynamic), and the direction and absence of gravitational acceleration, on particle collision, agglomeration and breakup, and fluid turbulence, in vertical channel flows has been investigated. Large eddy simulation, discrete particle simulation, deterministic hard-sphere collision and energy-balanced based agglomeration models, and breakup due to hydrodynamic shear stress, were all adopted for this study. Due to the small particle Stokes number considered, inherent in a solid-liquid flow and small simulation time $\Delta t^* \sim 100$, only small effects were observed for the static versus dynamic particle size distribution on the fluid turbulence. In the vertical channel flow case, particles in downward and zero gravity flows are transported towards the wall where they accumulate, while particles in upward flow migrate away from the wall. This segregation pattern, as well as changes in the wall shear stresses and mass flow rate due to buoyancy effects, do affect the flow turbulence and the evolution of inter-particle collisions and the collision efficiency, as well as agglomerate breakup rate.

6 ACKNOWLEDGEMENTS

The authors would also like to thank the EPSRC for their support of the DISTINCTIVE (Decommissioning, Immobilisation and Storage Solutions for Nuclear Waste Inventories) Consortium under grant EP/L014041/1 which supported the work described.

REFERENCES

[1] Yamamoto, Y., Potthoff, M., Tanaka, T., Kajishima, T. and Tsuji, Y. Large-eddy simulation of turbulent gas–-article flow in a vertical channel: Effect of considering inter-particle collisions. *J. Fluid Mech.* (2001) **442**:303-334.

[2] Njobuenwu, D.O. and Fairweather, M. Simulation of turbulent particulate flows for nuclear waste management: Agglomeration in vertical flows. In *Computer Aided Chemical Engineering* 38, Zdravko, K. and Miloš, B. (Eds). Elsevier (2016).

[3] Marchioli, C., Picciotto, M. and Soldati, A. Influence of gravity and lift on particle velocity statistics and transfer rates in turbulent vertical channel flow. *Int. J. Multiphase Flow* (2007) **33**:227-251.

[4] Molin, D., Marchioli, C. and Soldati, A. Turbulence modulation and microbubble dynamics in vertical channel flow. *Int. J. Multiphas. Flow* (2012) **42**:80-95.

[5] Njobuenwu, D.O. and Fairweather, M. Deterministic modelling of particle agglomeration in turbulent flow. In *Eighth International Symposium on Turbulence, Heat and Mass Transfer*, Sarajevo (2015), 587-590.

[6] Njobuenwu, D.O. and Fairweather, M. Simulation of deterministic energy-balance particle agglomeration in turbulent liquid-solid flows. *arXiv preprint arXiv:1701.02346* (2017).

[7] Babler, M.U., Biferale, L., Brandt, L., Feudel, U., Guseva, K., Lanotte, A.S., Marchioli, C., Picano, F., Sardina, G., Soldati, A. and Toschi, F. Numerical simulations of aggregate breakup in bounded and unbounded turbulent flows. *J. Fluid Mech.* (2015) **766**:104-128.

[8] Piomelli, U. and Liu, J. Large-eddy simulation of rotating channel flows using a localized dynamic model. *Phys. Fluids* (1995) **7**:839-848.

[9] Njobuenwu, D.O. and Fairweather, M. Simulation of inertial fibre orientation in turbulent flow. *Phys. Fluids* (2016) **28**:063307.

[10] Mei, R. An approximate expression for the shear lift force on a spherical particle at finite reynolds number. *Int. J. Multiphas. Flow* (1992) **18**:145-147.

[11] Sundaram, S. and Collins, L.R. Numerical considerations in simulating a turbulent suspension of finite-volume particles. *J. Comput. Phys.* (1996) **124**:337-350.

[12] Breuer, M. and Almohammed, N. Modeling and simulation of particle agglomeration in turbulent flows using a hard-sphere model with deterministic collision detection and enhanced structure models. *Int. J. Multiphas. Flow* (2015) **73**:171-206.

[13] Bini, M. and Jones, W. Particle acceleration in turbulent flows: A class of nonlinear stochastic models for intermittency. *Phys. Fluids* (2007) **19**:035104.

[14] Marchioli, C. and Soldati, A., Reynolds number scaling of particle preferential concentration in turbulent channel flow. In *Advances in Turbulence XI*. 117, Palma, J. M. L. M. and Lopes, A. S. (Eds). Springer (2007).

[15] Pang, M., Wei, J. and Yu, B. Effect of particle clusters on turbulence modulations in liquid flow laden with fine solid particles. *Braz. J. Chem. Eng.* (2011) **28**:433-446.